Synthesis, Characterization, and UV Curing Kinetics of Hyperbranched Polycarbosilane

Sheng-Jie Wang, Xiao-Dong Fan, Jie Kong, Yu-Yang Liu

Department of Applied Chemistry, School of Science, Northwestern Polytechnical University, Xi'an 710072, People's Republic of China

Received 12 April 2007; accepted 18 October 2007
DOI 10.1002/app.27534
Published online 6 December 2007 in Wiley InterScience (www.interscience.wiley.com).

ABSTRACT: Hyperbranched polycarbosilane with allyl end groups was synthesized via hydrosilylation of methyldiallyldilane, and characterized by Fourier transform infrared spectroscopy, ^{1}H, ^{13}C, ^{29}Si nuclear magnetic resonance, and size exclusion chromatography/multiangle laser light scattering. The degree of branching and average number of branches of the resulted polymer determined by ^{29}Si NMR spectroscopy is 0.58 and 0.42, and the exponent α in Mark–Houwink equation is 0.33 based on the relationship between viscosity and molecular weight. UV curing behaviors of the hyperbranched polycarbosilane were investigated using differential scanning photocalorimeter, and the effects of diluent's concentration, light intensity, reaction atmosphere, and temperature on the curing behaviors and kinetics were studied in detail. It was found that curing reaction can be accomplished rapidly under UV irradiation within 40 s both in air and in nitrogen atmosphere if acrylic reactive diluent was employed. The result suggests that it is an effective way to increase the curing reactivity by incorporating acrylic reactive diluents with high UV sensitivity into the polycarbosilane system. © 2007 Wiley Periodicals, Inc. J Appl Polym Sci 107: 3812–3822, 2008

Key words: hyperbranched; polycarbosilane; UV curing; kinetics; differential photo calorimeter

INTRODUCTION

Highly branched polymers as well as dendrimers and hyperbranched polymers are attracting great attentions from polymer scientists recently due to their special molecular architectures, distinct physical properties, and potential industrial applications in coating, additives, drug and gene delivery, macromolecular building blocks, nanotechnology, and supramolecular science.[1–9] Dendrimers with highly regular structures and well-controlled molecular weights are usually synthesized by multistep reactions with tedious isolation and purification procedures. Hyperbranched polymers, possessing a little lower degree of branching (DB) and broader molecular weight distributions compared to dendrimers, can be prepared in a one-step synthesis approach, which can reduce the cost and environment pollution. Therefore, hyperbranched polymers, such as hyperbranched organosilicon polymers, hyperbranched polyphenylenes, hyperbranched polyester, hyperbranched polyether, hyperbranched polyurethane, hyperbranched poly(ether ketone)s, show potentials for both laboratory and commercial preparations.[10–14]

As well known, it is a competent approach to prepare high performance ceramics via pyrolysis of polymer precursors including polysilazane, polycarbosilazane, and polycarbosilane with inorganic skeletons.[15–18] Hyperbrcnched polycarbosilane can be regarded as a kind of potential precursors due to its unique structure and favorable properties, such as lower viscosities, favorable solubility, and large quantity of end functional groups. Particularly, photopolymerization including UV irradiation over polycarbosilane can be applied to fabricate the ceramic parts with complex structures and shapes by less processing steps or free mould process if incorporating photocrosslinkable groups. As we know, polycarbosilane precursors with vinyl or allyl end groups can be prepared expediently. However, even with large amounts of photoinitiator or at high temperature, the photocrosslinking speed of these precursors is lower than that of other typical UV-curable polymers, such as acrylates and methacrylates.[19–21] Therefore, how to increase the UV curing speed of these precursors is one of the important issues for improving the process of fabrication ceramic apparatuses.

It may be an effective way to increase its curing speed by incorporating acrylic reactive diluents into

Correspondence to: X. D. Fan (xfand@126.com).

Contract grant sponsor: Northwestern Polytechnical University Scientific and Technological Innovation Foundation; contract grant number: M450211.

Contract grant sponsor: National Natural Science Foundation of China; contract grant number: 2060419.

Contract grant sponsor: Natural Science Basic Research Project of Shaanxi Province; contract grant number: 2006B15.

the polycarbosilane system, which may result in copolymerization of allyl (or vinyl) groups with acrylic groups. In this article, hyperbranched polycarbosilane with allyl end groups was synthesized firstly, and then reactive diluent, tripropane glycol diacrylate (TPGDA) was introduced. The curing reaction can be carried out rapidly when TPGDA was added. Subsequently, effects of the factors, including reactive diluent's concentration, light intensity, reaction atmosphere, and temperature on the curing behavior and kinetics were well studied.

EXPERIMENTAL

Materials

Methyldichlorosilane (industry grade, more than 98% purity) was purchased from Zhejiang Xin'an Chemical, China; allyl chloride (analytical grade) was purchased from Guoyao Chemical Regents Centre, China; chloroplatinic acid (analytical grade) was provided by Shannxi Kaida Chemical, China; IHT-PI 185 (2-hydroxy-2-methyl-1-(4-tertbutyl) phenyl-propane-1-one) was obtained from Insight High Technology, China; TPGDA was obtained from Guangzhou Hongyun Polymer Materials Corporation in China; tetrahydrofuran (analytical grade), magnesium (analytical grade), and other solvents were obtained from Tianjin Kermel Chemical Reagents Development Center, China. Silane monomer and all the solvents were distilled and dried with 4 Å grade molecular sieve before use.

Synthesis

Synthesis of methyldiallylsilane

Magnesium (10.56 g, 0.44 mol) and dry THF (200 mL) were charged into a four-necked flask equipped with a mechanical stirrer, a reflux condenser, a nitrogen inlet, and a dropping funnel, and then the mixture was raised to 55°C. A solution of allyl chloride (33.7 g, 0.44 mol) and methyldichlorosilane (23.0 g, 0.2 mol) in 50 mL of dry tetrahydrofuran was then added at a rate of 30 drops per minute. The reaction system was kept at a modest reflux for 24 h. Then the mixture was cooled to ambient temperature. The precipitated magnesium salts formed in the reaction were filtered off, and then the solvent was evaporated. The residue was distilled under reduced pressure at 47°C/−0.85 MPa. Methyldiallylsilane was obtained as colorless liquid (yield: 37%).

FTIR (cm^{-1}, KBr): 3082 (=C—H), 2110 (Si—H), 1631 (C=C), 1253 (Si—CH_3); ^{1}H NMR (ppm, $CDCl_3$): 5.61–5.76 (—CH_2—C*H*=CH_2, 2H), 4.75–4.78 (—CH_2—CH=C*H*$_2$, 4H), 3.70–3.73 (Si—*H*, 1H), 1.52–1.54 (—C*H*$_2$—CH=CH_2, 4H), −0.01−0.00 (Si—C*H*$_3$, 3H); Elemental analysis: Calcd for $C_7H_{14}Si$: C 66.67 %, H 11.11%. Found: C 66.62%, H 11.14%.

Synthesis of hyperbranched polycarbosilane

The Karstedt catalyst was prepared according to the synthetic procedures described in reference.[22]

Karstedt catalyst (10 mg) was added to the solution of methyldiallylsilane (12.6 g, 0.1 mol) and anhydrous tetrahydrofuran (20 mL). The mixture was kept at 50°C under vigorous magnetic stirring until no silicon hydride groups were detected in FTIR spectra (2110 cm^{-1}, typically 4 h). The product was distilled under reduced pressure to remove solvent, and then was kept at 50°C/−0.1 MPa for 12 h, thus hyperbranched polycarbosilane was obtained as light yellow viscous liquid.

FTIR (cm^{-1}, KBr): 3078 (=C—H), 2915 (—CH_3), 1633 (C=C), 1254 (Si—CH_3); ^{1}H NMR (ppm, $CDCl_3$): 5.74–5.83 (—CH_2—C*H*=CH_2), 4.81–4.89 (—CH_2—CH=C*H*$_2$), 1.52–1.55 (—C*H*$_2$—CH=CH_2), 1.36–1.44 (Si—CH_2C*H*$_2$$CH_2$—Si, β addition product), 0.95–1.01 (Si—CH(C*H*$_3$)CH_2—Si, α addition product), 0.58–0.66 (Si—C*H*$_2$$CH_2$C*H*$_2$—Si, β addition product), 0.00–0.08 (Si—C*H*$_3$); ^{13}C NMR (ppm, $CDCl_3$): 134.8–135.2 (—CH_2—C*H*=CH_2), 112.6–113.2 (—CH_2—CH=C*H*$_2$), 21.6–22.2 (—C*H*$_2$—CH=CH_2), 18.0–19.0 (Si—C*H*$_2$$CH_2$C*H*$_2$—Si), −5.6–4.8 (Si—C*H*$_3$).

Instrumentation

^{1}H NMR, ^{13}C NMR, and ^{29}Si NMR measurements were conducted on Bruker AV-500 at 25°C, using $CDCl_3$ as solvent, and tetramethylsilane as internal standard. Elemental analysis was performed on a Vario (the United States) ELIII instrument. SEC/MALLS analysis was carried out on a size exclusion chromatography (SEC)/multiangle laser light scattering (MALLS) instrument (Wyatt Technology, St. Barbara, CA). The chromatographic system consists of a Waters 515 pump, an auto sampler, a differential refrectometer (Optilab rEX), and two columns, MZ 10^3 Å (300 × 6.8 mm^2) and MZ 10^4 Å (300 × 6.8 mm^2). The columns were kept at 25°C in a thermostat. HPLC grade tetrahydrofuran was used as solvent with a flow rate of 1.0 mL/min. MALLS detector (DAWN EOS) and differential viscosity meter (ViscoStar) were placed between the SEC and the refractive index detector (Optilab rEX, Wyatt Technology, St. Barbara, USA). ASTRA software (Version 5.1.3.0) was used for data acquisition and analysis. Differential scanning photo calorimeter (DPC) measurements were conducted on a differential scanning calorimeter (MDSC 2910, Waters-TA instrument, USA) equipped with a photo calorimeter accessory (Novacure 2100, EXFO Photonic Solutions). The light source was a 100 W middle-pressure mercury lamp.

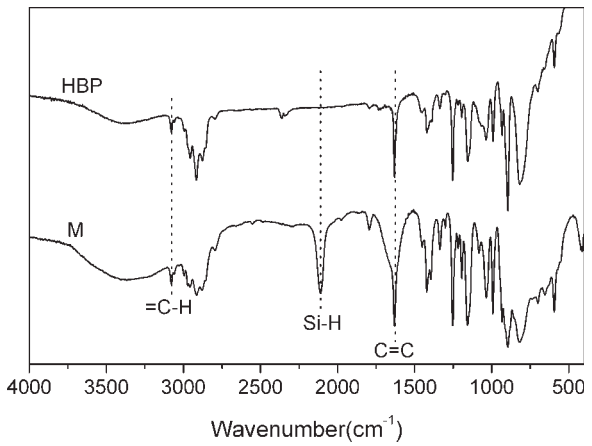

Figure 1 FTIR spectra of monomer and polymer.

The UV light exposure intensity was set as 19.4, 38.8, 63.8, 80.4, and 99.8 mW/cm^2 (the light source at a distance of 20 mm from the sample, the actual light intensity exposed on specimens is $\sim$ 10% of the set)[23] over a wavelength range of 320–500 nm. The samples (weight 1.5 $\pm$ 0.5 mg) were placed in uncovered aluminum pans, with a distance of 20 mm from the UV source to the specimen. FTIR spectra were obtained on a WQF-310 model, Rui Li Beijing, China, using KBr as the sample holder. The scanning range was set from 4000 cm^{-1} to 400 cm^{-1}. TGA (Q-50, Waters-TA Instruments, USA) measurements were used to determine the thermal stability of the UV cured polymer, and the heating rate was set as 20°C /min within the temperature range of 30–800°C.

RESULTS AND DISCUSSION

Synthesis and characterization of methyldiallylsilane

Methyldiallylsilane was synthesized via allylation reaction of methyldichlorosilane and allyl chloride. Allylation reaction can usually be carried out through two steps approach: first, allylmagnesium chloride as Grignard reagent is prepared, and second substituent reaction is conducted.[24,25] In this study, allylation reaction can be accomplished only using one step in which chlorosilane and allyl chloride are added together into a mixture of magnesium and tetrahydrofuran at 55°C in dry nitrogen atmosphere. It is found that the allylation reaction conducted in this research possesses a shorter induction period compared with the two steps approach, and the reaction can be performed smoothly all along by carefully controlling the reagent feeding rate. The vibration peak at 1631 cm^{-1} in FTIR spectrum (Fig. 1 M) is found, and the resulting methylene segment bonded silicon atom (Si—CH_2—CH=CH_2) are also presented at the chemical shift position of 1.52–1.54 ppm in its ^{1}H NMR spectrum [Fig. 2(a)].[26] Furthermore, elemental analysis also indicates that the designed methyldiallylsilane has been obtained successfully.

Synthesis and characterization of hyperbranched polycarbosilane

^{1}H NMR

The hyperbranched polycarbosilane was synthesized via hydrosilylation reaction of methyldiallylsilane catalyzed by Karstedt catalyst. The vibration peak at 2110 cm^{-1} for Si—H groups disappears in FTIR spectrum (Fig. 1 HBP) of the resulted polymer, while the vibration peak at 1633 cm^{-1} for C=C groups can still be observed. Furthermore, the methylene segments resulting from hydrosilylation can also be confirmed by two new peaks occurring at the chemical shift position of 1.36–1.44 ppm and 0.58–0.66 ppm [Fig. 2(b)], which are responding to (Si—$CH_2CH_2CH_2$—Si) and (Si—$CH_2CH_2CH_2$—Si), respectively. On the other hand, the molecular structure of the polymer is also proved by its ^{13}C NMR spectrum as presented in Figure 3. It should be pointed out that hydrosilylation reaction often produces α and β addition products. The chemical shift

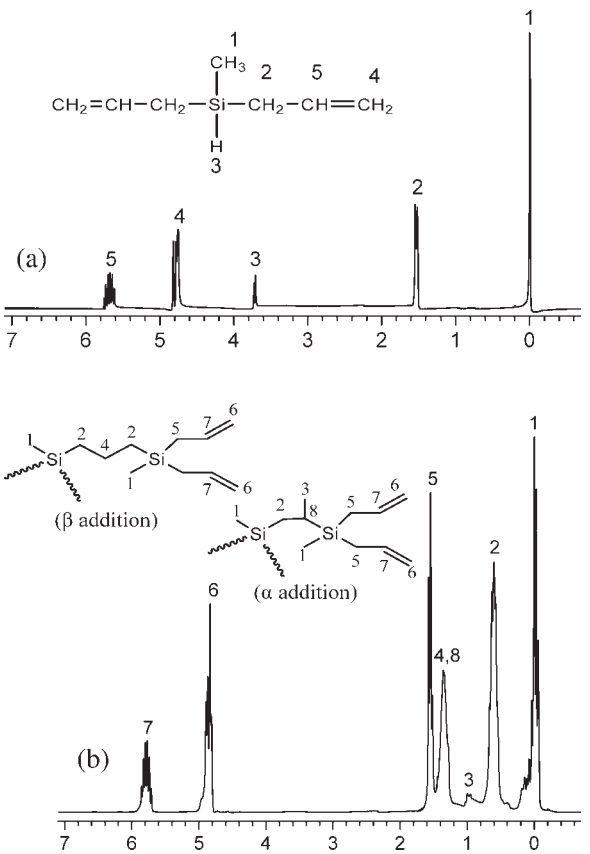

Figure 2 ^{1}H NMR spectra of monomer (a) and polymer (b).

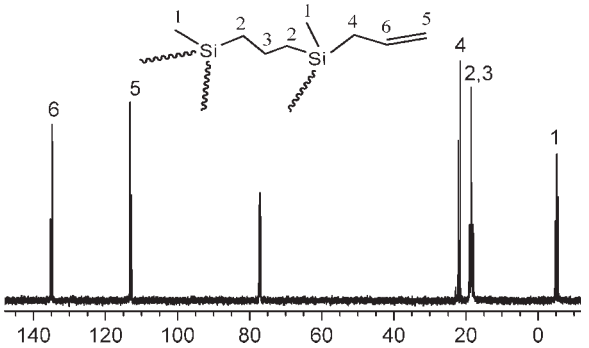

Figure 3 ^{13}C NMR spectrum of polymer.

at 0.98–1.01 ppm in ^{1}H NMR spectrum of polymer [Fig. 2(b)] can be assigned to the methyl group resulting from α addition, whereas β addition gives rise to the chemical shift at 0.58–0.66 ppm.[24] Relative integration of α and β addition signals implies that the hydrosilylation reaction in such conditions yields mainly β addition product, which can accounts for over 98%.

^{29}Si NMR

If we presume no molecular internal cyclization and other side reactions occurring in the polymerization process, the silicon atoms in main chain can carry different number of allyl groups. We can see that there are only just three chemical shifts in ^{29}Si NMR spectrum (Fig. 4). According to Refs. 27, 28 the chemical shift at 0.98 ppm can be contributed to the silicon atoms without allyl groups. Considering the influences of substituent groups on chemical shift in ^{29}Si NMR spectrum,[29–31] the chemical shifts at 0.67 ppm and 0.18 ppm can be assigned to the silicon atoms linked one and two allyl groups, respectively. As presented in Figure 4, silicon atoms linked zero, one, and two allyl groups are labeled as Si^{D}, Si^{L}, and Si^{T}, which also represents dendritic, linear, and terminal branch points, respectively. The relative area integration ratio of Si^{D}, Si^{L}, and Si^{T} in Figure 4 is 1 : 1.39 : 0.66, and then the DB and the average number of branches (ANB) of the hyperbranched polycarbosilane can be obtained according to the following equations[32]:

$$\mathrm{DB} = \frac{2D}{2D + L} \tag{1}$$

$$\mathrm{ANB} = \frac{D}{D + L} \tag{2}$$

where D and L represent the fractions of dendritic and linear units in the resulted hyperbranched polymers obtained from integration of the respective signals in Figure 4. According to the above equations, the value for DB and ANB is calculated as 0.58 and 0.42, respectively.

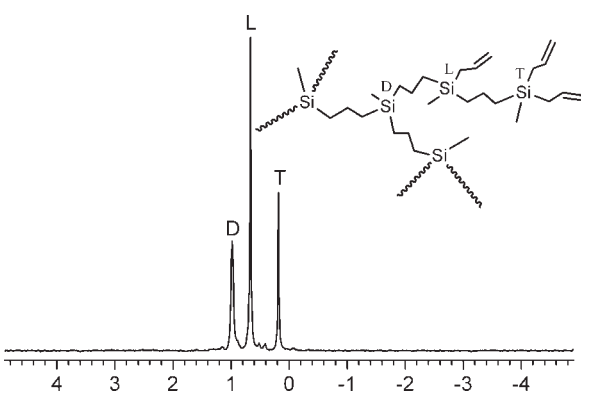

Figure 4 ^{29}Si NMR spectrum of polymer.

SEC/MALLS

Molecular weight and molecular weight distribution for linear polymers are usually determined via SEC technology by using linear polymer calibration standard. In SEC measurements, polymers are fractionated according to their hydrodynamic volume. However, for hyperbranched polymers, their sphere like shapes rather than random coil results in less entanglement between molecules, so their molecular sizes are smaller than that of linear ones with the same molecular weight.[33] Light scattering (LS) is the most widely used technique for determining the absolute molecular weight without requiring any calibration.[34] Simultaneous measurement of LS intensity and concentration allows direct determination of the weight average molecular weight for each eluted fraction without calibration by using standard materials.[35] SEC coupled with MALLS and viscometer is employed to determine molecular structure parameters of hyperbranched polycarbosilane in this article. Elution curves of hyperbranched polymer are presented in Figure 5. The weight average molecular

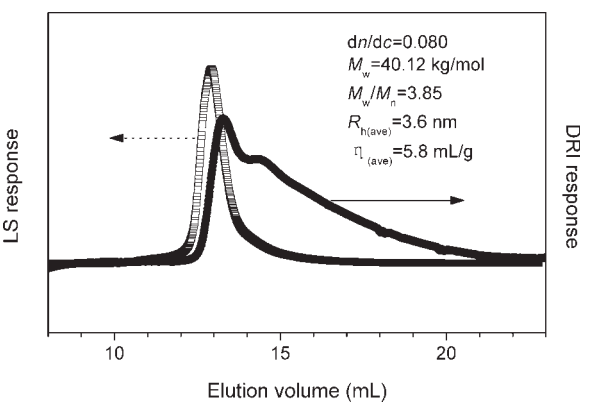

Figure 5 SEC elution curves of hyperbranched polycarbosilane with different detector.

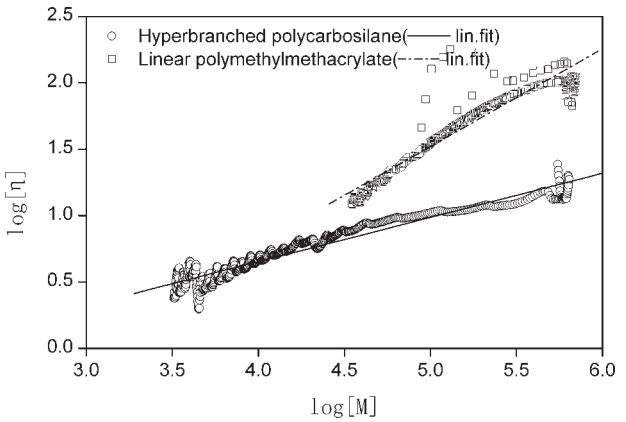

Figure 6 MH plots for hyperbranched polycarbosilane and linear polymethylmethacrylate.

weight (M_w) is determined as 40.12 kg/mol, with a polydispersity of 3.85. It is interesting that DRI and LS responses of the polymer are not synchronous. Similar phenomena can also be found in other polymers, such as polyethylene[36] and hyperbranched polycarbosiloxane.[35] This is attributed to the existence of large amounts of low molecular weight fractions in the hyperbranched polycarbosilane. It is well known that LS response is more sensitive to the fraction with high molecular weight, while DRI response is proportional to the concentration of elution fractions. Fractions with higher molecular weight are firstly eluted from chromatographic column at very low concentration, which can just be observed in LS response. Subsequently, lower molecular weight fractions with high concentration eluted, and their intensity in DRI response increases at a higher speed compared with LS response. Thus the DRI response is behind the LS response in the elution curve of hyperbranched polycarbosilane.

Relationship between the intrinsic viscosities and molar masses of the polymer can be used to evaluate their molecular shapes. According to Mark–Houwink (MH) equation, the dependence of the intrinsic viscosity of a polymer on its molar mass is given as follows:

$$[\eta] = \mathrm{K}\mathrm{M}^{\alpha} \tag{3}$$

The exponent α in MH equation depends on the molecular structure. Hard spheres give values of nearly zero, rigid rods give values ranging from 1 to 2, linear polymers exhibiting random coil structures give values ranging from 0.5 to 0.7, and hyperbranched polymers often give values below 0.5 except for connecting the polar end groups that can cause a strong interaction with the solvent and thus, an expansion of the molecular structure.[37–39] MH plots for hyperbranched polycarbosilane are shown in Figure 6. For comparison, the double logarithmic plots for linear polymethylmethacrylate are also depicted. As seen in Figure 6, it is obvious that the slope of the linear fit of MH plots for linear polymethylmethacrylate is higher than that for hyperbranched polycarbosilane. The exponent α for hyperbranched polycarbosilane is calculated as 0.33, which indicates, as expected, there is a relatively compact arrangement corresponding to its hyperbranched structure.

UV curing behavior of hyperbranched polycarbosilane

The UV-curable polymer system consists of hyperbranched polycarbosilane, photoinitiator of 2-hydroxy-2-methyl-1-(4-tertbutyl)-phenyl-propane-1-one (IHT-PI 185), and acrylic reactive diluent of TPGDA. The UV curing is monitored using DPC. In the DPC methodology, the heat flow is assumed proportional to the conversion rate during curing. Therefore the rate of conversion (R_p) can be defined as follows[40,41]:

$$R_p = \frac{d\alpha}{dt} = \frac{1}{\Delta H_{\mathrm{th}}}\frac{dH}{dt} \tag{4}$$

where $d\alpha/dt$ is the conversion rate or polymerization rate (R_p), dH/dt is the measured heat flow, and the theoretical enthalpy ΔH_{th} was calculated using Eq. (5) and taking into account polymerization enthalpy values of double bonds in allyl (84 kJ/mol) and acrylate (77.9 kJ/mol) groups.[42,43]

$$\Delta H_{\mathrm{th}} = w_1 f_1 \Delta H_{p1}/M_1 + w_2 f_2 \Delta H_{p2}/M_2 \tag{5}$$

where w is mass concentration of each compound in the curing system, f is the average functionality, ΔH_p is polymerization enthalpy, M is the average molecular weight. For the hyperbranched polycarbosilane synthesized from AB_2 monomers, there are one molar residual allyl groups every molar monomer's weight if all the A group was exhausted during the reaction with B. The degree of conversion is calculated from the integrated form of Eq. (4)

$$\alpha_t = \frac{\Delta H_t}{\Delta H_{\mathrm{th}}} \tag{6}$$

where α_t is the degree of conversion at time t and ΔH_t is the cumulative heat of reaction up to time t.

The influence of TPGDA content, reaction atmosphere, light intensity, and reaction temperature on UV curing behaviors of hyperbranched polycarbosilane system was discussed as follows.

Influence of TPGDA content

It is well known that the radical polymerization reactivity of allyl groups is lower compared with acrylic

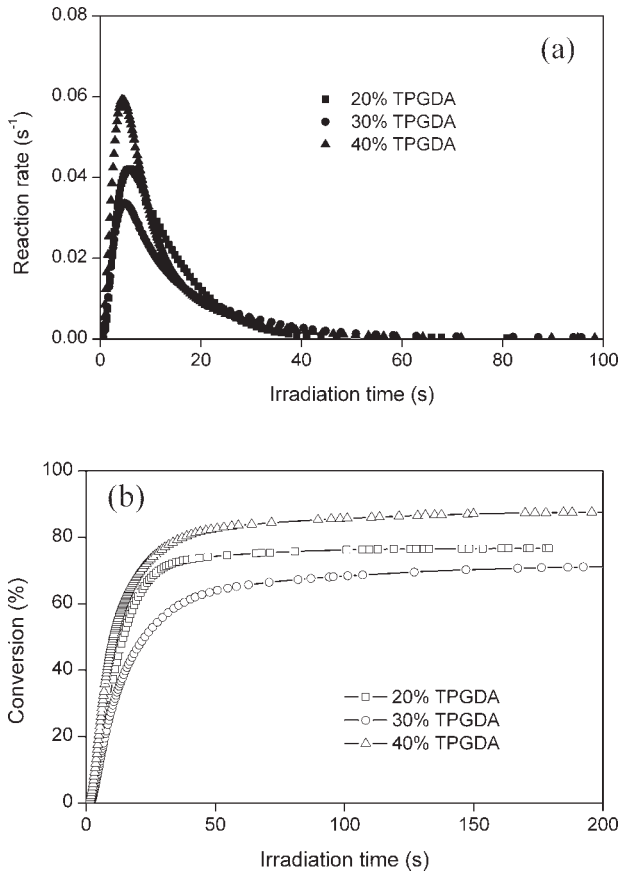

Figure 7 Reaction rate–time (a) and conversion–time (b) curves for polycarbosilane system with different TPGDA content in nitrogen. Light intensity 38.8 mW/cm^2, and isothermal curing at 20°C.

groups. Either in nitrogen or in air atmosphere, with light intensity of 38.8 mW/cm^2, no reaction phenomena can be observed at 20°C when the system just consisting of hyperbranched polycarbosilane and 4 wt % photoinitiator. However, the UV curing reaction can be well performed if introducing acrylic compound into the system. Figure 7 shows the reaction rate–time and conversion–time curves of the polycarbosilane system with different TPGDA content in nitrogen, and the detailed curing parameters, such as the t_i (the time to attain 1% of conversion), a_f (the final conversion), and t_p, R_p, and α_p (the time, rate, and conversion at the maximum polymerization rate, respectively), are listed in Table I. From the shape of reaction rate–time curves in Figure 7(a), it can be found that there is only one exothermic peak during the UV curing process of polycarbosilane system. Besides, it can be judged from the final exothermic heat that most of allyl and acrylate groups took part in the curing reaction. So it is concluded that radical copolymerization reaction between allyl and double bonds of acrylic compound may be occurred during the curing process. From Figure 7 and Table I, it can be found that the reaction rate and conversion of the UV curing system with 40 wt % TPGDA is higher than that with 20 or 30 wt % TPGDA. This is due to the reactivity improves with the content of high reactive groups increased.

The reaction rate–time and conversion–time curves of polycarbosilane system with different TPGDA content in air atmosphere are shown in Figure 8, and the detailed curing parameters are listed in Table I. As we know that reaction atmosphere can influence the radical reaction, inhibition effect of oxygen in air can also be observed in this investigation. However, in air atmosphere, it is interesting that the curing reaction rate and final conversion decrease with increase of TPGDA content, which is different from that curing in nitrogen atmosphere. This result may be attributed to the inhibition effect of oxygen. The viscosity of the curing system falls with the increase of TPGDA content, which allows larger quantity of oxygen penetrating into the curing system and diffusing at a faster speed, resulting in the increase in inhibition effect of oxygen. Thus, the reaction rate and conversion decreases with TPGDA increasing. Considering the thermal stability falling with TPGDA content increased, as described in the subsequent discussion, the reactive diluent's content is set as 20 wt % in the following part of this investigation.

Influence of light intensity

In the presence of TPGDA (20 wt %), isothermal DPC measurements are carried out at 20°C with light intensity of 19.4–99.8 mW/cm^2. Reaction rate versus irradiation time in nitrogen and air atmos-

TABLE I
UV Curing Parameters of Polycarbosilane Systems with Different TPGDA Content

Item	Atmosphere	t_i (s)	t_p (s)	$R_p \times 100$ (s^{-1})	$\alpha_p \times 100$	$\alpha_f \times 100$
20% TPGDA	N_2	2.21	5.86	4.22	13.43	63.62
	Air	7.12	10.87	1.25	5.07	35.24
30% TPGDA	N_2	2.04	4.88	3.53	9.11	62.14
	Air	7.16	10.52	0.92	3.77	20.46
40% TPGDA	N_2	1.53	4.35	6.51	14.67	79.83
	Air	9.10	11.37	0.60	2.29	17.87

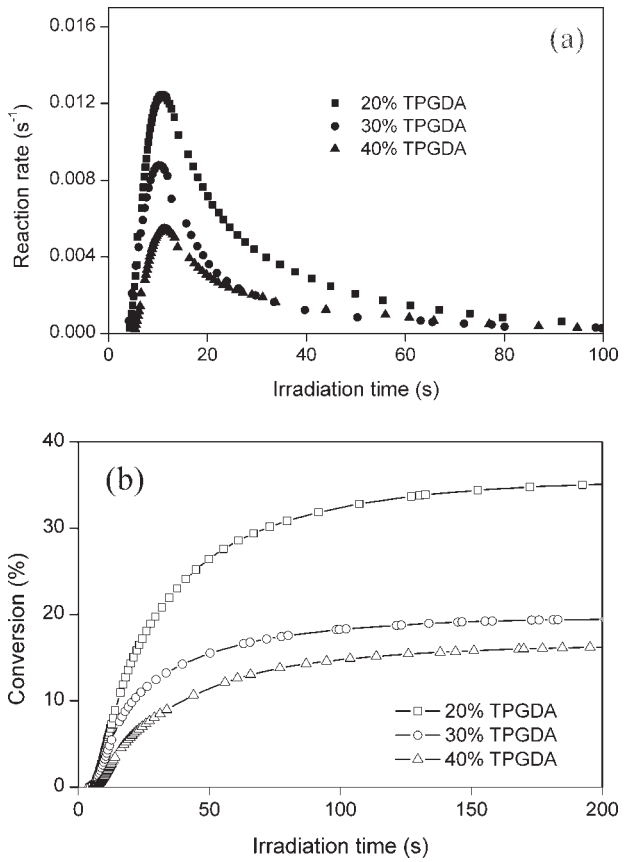

Figure 8 Reaction rate–time (a) and conversion–time (b) curves for polycarbosilane system with different TPGDA content in air. Light intensity 38.8 mW/cm^2, and isothermal curing at 20°C.

phere are shown in Figure 9, and the curing parameters are collected in Table II. It is found that the reaction rate increases with the increase of light intensity in either nitrogen or air atmosphere [Fig. 9(a)]. This may be explained by the free volume effect.[44,45] The initiation rate is very high in the photoinitiated polymerization, and crosslinking systems cannot be in volume equilibrium because volume shrinkage rate is much slower than chemical reaction rate. This results in a temporary excess of free volume which increases the mobility of the residual double bonds and active centers. Thus, the higher the light intensity is, the higher the polymerization rate can be attained. There are similar trends on the final conversion (Table II). In nitrogen atmosphere, the final conversion increases with the increase of irradiation intensity until it reaches the maximum value at 80.4 mW/cm^2. This result may be attributed to the conjunct effects of free volume effect and glass effect.[44–46] Just as excess free volume allows high conversion, the onset of vitrification of the curing system will be brought forward with the reaction rate increased as a consequence of increasing light intensity, in which the curing reaction becomes diffusion controlled at a comparatively low conversion. Therefore, the final conversion decreases when the light intensity exceeds a certain value. As shown in Figure 9, the reaction in air atmosphere starts after an obvious inhibition period. The induction time decreases with increasing light intensity. This indicates that the inhibition effect of oxygen can be diminished by increasing light intensity.

Figure 10 presents reaction rate-square root of light intensity curves at a conversion of 5%. The linear relationship in either nitrogen or air atmosphere can be found, which is well in accordance with the following equation[46]:

$$R_{\mathrm{P_i}} = -\frac{d[M]}{dt} = \frac{k_p}{k_t^{0.5}}[M](\phi\varepsilon[A]_0)^{0.5}(I_0)^{0.5} \qquad (7)$$

where R_{pi} is the reaction rate at the beginning of the reaction, k_p and k_t are the propagation and termination rate constants, $[M]$ is the molar concentration of double bonds, φ is the quantum yield, ε is the photoinitiator molar extinction coefficient, $[A]_0$ is the initial concentration of photoinitiator, and I_0 is the initial light intensity. Besides, it can be found that

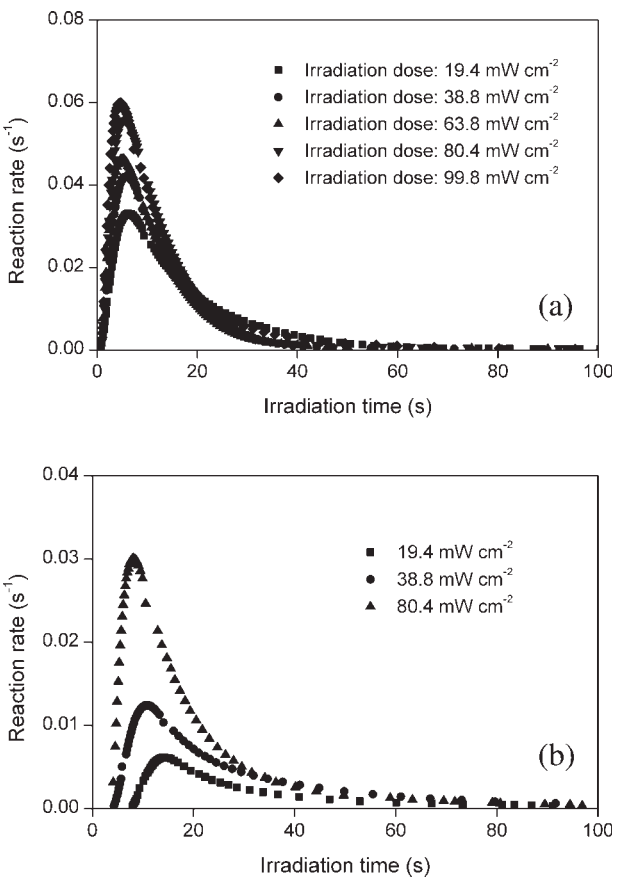

Figure 9 Reaction rate–time curves with different light intensity in nitrogen (a) and air (b) atmosphere.

TABLE II
UV Curing Parameters of Polycarbosilane Systems with Different Light Intensity

Light intensity (mW/cm^2)	Atmosphere	t_i (s)	t_p (s)	$R_p \times 100$ (s^{-1})	$\alpha_p \times 100$	$\alpha_f \times 100$
19.4	N_2	2.44	6.75	3.30	11.80	57.70
	Air	11.76	14.33	0.61	2.49	17.08
38.8	N_2	2.20	5.86	4.22	13.43	63.62
	Air	7.12	10.87	1.25	5.07	35.24
63.8	N_2	1.85	5.17	4.63	14.24	69.15
80.4	N_2	2.00	5.38	5.58	14.65	71.78
	Air	6.31	8.13	3.00	8.32	52.95
99.8	N_2	1.96	4.72	6.00	13.18	67.54

the fitting curve in air has a higher slope compared with that in nitrogen, which suggests that initiation activity of polycarbosilane system in air is more sensitive to the changes of light intensity than in nitrogen.

Influence of reaction temperature

The influence of temperature on UV curing reaction for polycarbosilane system is studied at presence of 20 wt % TPGDA. The light intensity is set as 38.8 mW/cm^2. Figure 11 shows the conversion versus irradiation time at different temperature in nitrogen (a) and in air (b) atmosphere, respectively. The detailed curing parameters obtained from Figure 11 are listed in Table III. In Figure 11, it predicts that the final conversion increases with raising the reaction temperature that has been found in other thermosetting systems.[45] This increase in conversion is mainly attributed to the increased mobility of the reactive species. It is noteworthy that the final conversion cured in air [Fig. 11(b)] at 0°C is only 8.72%, lower than that of other reactions at a large extent. As we know, some of free radicals will be consumed by oxygen. Moreover, the mobility of radical species drops with the decrease of the reaction temperature. All of them can result in lower final conversion as shown in Figure 11(b).

From Table III, the maximum reaction rate versus temperature and induction time versus temperature curves are obtained (Figure 12). Reaction performed in air has longer induction times compared with that in nitrogen. In air atmosphere, the induction time reduces with raising the reaction temperature. However, in nitrogen atmosphere, there are no obvious changes in induction time with the increase of temperature. This result can be explained as the induc-

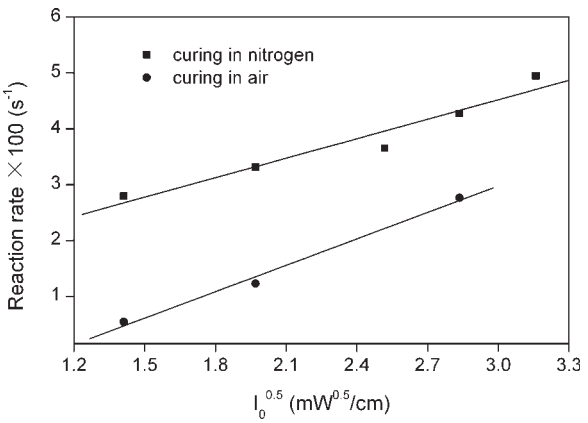

Figure 10 Reaction rate-square root of light intensity curves at the conversion of 5%.

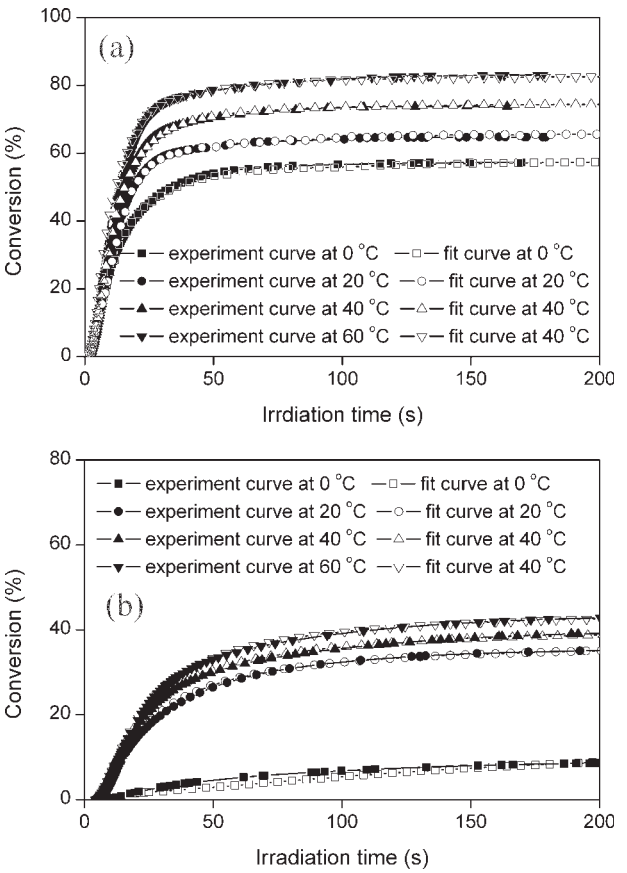

Figure 11 Comparison of experimental data with Kamal model at different temperature in nitrogen (a) and air (b) atmosphere. Conversion versus time.

TABLE III
UV Curing Parameters of the Polycarbosilane System at Different Temperature

Temperature (°C)	Atmosphere	t_i (s)	t_p (s)	$R_p \times 100$ (s^{-1})	$\alpha_p \times 100$	$\alpha_f \times 100$
0	N_2	2.03	4.95	3.74	9.77	57.26
	Air	15.11	12.47	0.17	0.56	8.72
20	N_2	2.19	5.86	4.22	13.43	63.62
	Air	7.10	10.87	1.25	5.07	35.24
40	N_2	2.19	7.09	4.52	18.31	73.81
	Air	6.91	11.92	1.34	6.84	39.40
60	N_2	2.25	6.69	5.00	18.51	83.00
	Air	6.67	12.00	1.44	7.58	43.00

tion time is mainly caused by inhibition effect of oxygen. From Figure 12, it can also be found that the maximum reaction rate increases as the increase of reaction temperature. It is interesting that there is a linear relationship between the maximum reaction rate and temperature when the reaction is performed in nitrogen atmosphere, while the R_p-temperature plot is curved in air. The slope of the curve in air decreases with increasing the reaction temperature. As described above, the mobility of radical species increases for the enhancement of reaction temperature, which leads to high reaction rate. However, the viscosity of the curing system decreases with the increasing temperature, which leads to larger quantity of oxygen penetrating into the curing system and diffusing at a faster speed, resulting in decrease in reaction rate. Thus, the result shown in Figure 12 is the equilibrium of the two effects.

Investigation of UV curing kinetics

As shown in Figures 7–9 and Figure 11, a typical characteristic can be found. After irradiation for a few seconds, the auto-accelerative gel effect occurs that means the restricted segmental movement of radicals and diffusion-controlled termination. In this stage, k_t in Eq. (7) decreases, which results in a dramatic increase in R_p. Continuing the reaction, the viscosity of the system increases which leading to the propagation reaction becomes diffusion controlled. At this stage, k_p in Eq. (7) also decreases resulting in a fall in R_p. This decline in R_p is called glass effect.[47] These types of processes are often described by the model developed by Kamal.[48,49] The model equation is shown as follows:

$$R_p = \frac{d\alpha}{dt} = k\alpha^m(\alpha_f - a)^n \tag{8}$$

where n is the reaction order exponent and m is the autocatalytic exponent, k is the reaction rate constant, α_f is the final conversion which is described as the ratio of the total exothermal heat of each reaction to the theoretical enthalpy with the same prescription. Thus, applying Eq. (8) to this system, kinetic parameters, such as k, m, and n, can be obtained using a least square regression method to fit our experimental data to the model (using the software of MatLab 7.1), and are listed in Table IV. Figure 11 presents the comparison between the experimentally data and the data obtained from graph plotted using the model given in Eq. (8). Excellent agreements are observed except for the curves obtained at 0°C. Deviations observed at 0°C may be attributed to the restricted mobility of radical species in such a low reaction temperature. The reaction rate constant, k, is a temperature dependent Arrhenius type constant:

$$k(T) = A\exp\left(\frac{-E_a}{RT}\right) \tag{9}$$

where A is the pre-exponential or frequency factor, E_a is the activation energy, R is the gas constant, and T is the absolute temperature. To obtain the value of E_a, Eq. (9) can be given as follows:

$$\ln k = \ln A - \frac{E_a}{RT} \tag{10}$$

On the basis of Eq. (10), the activation energy E_a is obtained by plotting ln$k$ versus $1/T$. As presented in

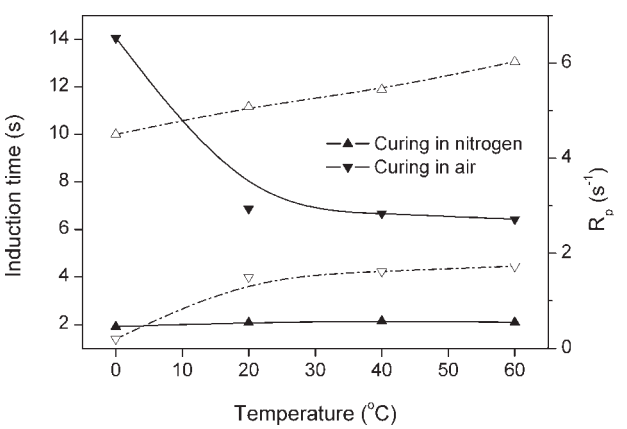

Figure 12 Reaction rate–temperature and induction time–temperature curves for the polycarbosilane system.

TABLE IV
UV Curing Kinetic Parameters of the Polycarbosilane System at Different Temperature

Atmosphere	Temperature (°C)	k (s^{-1})	m	n	Average of $m + n$	E_a (kJ/mol)	A (s^{-1})
N_2	0	0.1535	0.25	1.66	1.97	3.18	0.61
	20	0.1644	0.55	1.46			
	40	0.1741	0.45	1.44			
	60	0.2000	0.42	1.66			
Air	0	0.1189	0.63	1.55	2.21	3.22	0.49
	20	0.1285	0.23	1.89			
	40	0.1400	0.24	1.96			
	60	0.1537	0.34	2.01			

Figure 13, linear relationships are obtained, thus confirming the validity of the proposed model given in Eq. (8). The slope in nitrogen is close to that in air atmosphere, which indicates that there are no obvious influences of atmosphere on the curing reaction activation energy of polycarbosilane system. The activation energy E_a is calculated from the average of the two slopes, yielding a value of 3.2 kJ/mol.

Thermodegradation property of cured polycarbosilane systems

Samples for TGA test are prepared as following procedures: The liquid polycarbosilane systems including 4 wt % photoinitiator and different content of TPGDA are irradiated with a middle-pressure mercury lamp (400 W, HOK4/120 from Philips, Belgium) for 30 min, with a distance of 15 cm from lamp to specimen. And then the specimens are kept in a vacuum box (40°C, −0.1 MPa) for 4 h. Thus, homogeneous transparent solids for TGA test are obtained. Figure 14 presents the weight and weight loss rate curves of the cured polymers with different content of TPGDA. It can be seen that the maximum decomposition temperature for pure polycarbosilane system is about 480°C. However, for the cured polymers including TPGDA, they have additional weight loss peak centered at 375°C, and weight lost in this temperature reign increases with raising TPGDA content. Therefore, the polycarbosilane system with 20% TPGDA is chosen as the representative to investigate its UV curing behaviors as shown in the previous section.

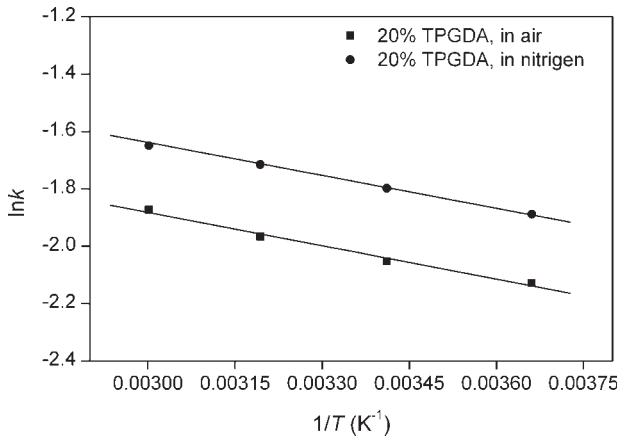

Figure 13 ln$k$ versus $1/T$ for polycarbosilane system in different reaction atmosphere.

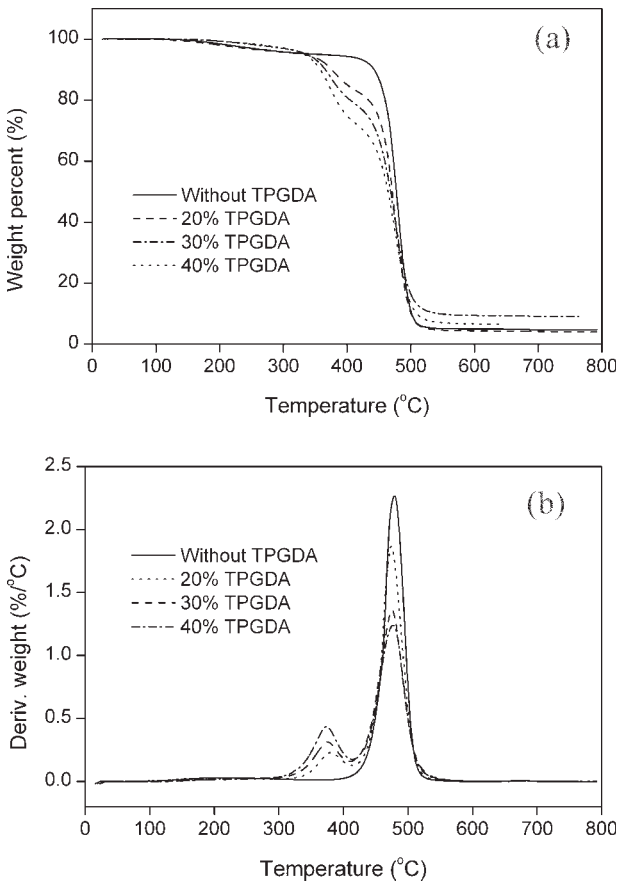

Figure 14 TGA (a) and DTG (b) curves of cured polycarbosilane systems with different TPGDA content.

CONCLUSION

Hyperbranched polycarbosilane containing allyl end groups was synthesized and characterized in detail. ^{29}Si NMR spectroscopy indicates that the DB and ANB of the hyperbranched polymer is 0.58 and 0.42, respectively. SEC/MALLS analysis shows that the exponent α in Mark–Houwink equation is 0.33. The resulted polycarbosilane can be cured rapidly under UV light irradiation if acrylic reactive diluent is incorporated into the UV curing system. DPC results indicates that the reaction rate and the final conversion decrease with increasing TPGDA content when the reaction is carried out in air atmosphere due to the influence of oxygen, and the inhibition effect of oxygen can be diminished by increasing light intensity. The reaction rate and final conversion increase with raising the temperature in either air or nitrogen atmosphere. The UV curing reaction activation energy E_a can be calculated as 3.20 kJ/mol by the kinetics analysis. Finally, TGA measurement suggests that thermostability of cured polycarbosilane decreases with enhancing the content of TPGDA.

References

1. Esumi, K. Top Curr Chem 2003, 227, 31.
2. Frey, H.; Lach, C.; Lorenz, K. Adv Mater 1998, 10, 279.
3. Gao, C.; Yan, D. Prog Polym Sci 2004, 29, 183.
4. Kim, Y. H. J Polym Sci Part A: Polym Chem 1998, 36, 1685.
5. Wei, H. Y.; Shi, W. F. Chem J Chin Univ 2001, 22, 338.
6. Bischoff, R.; Cray, S. E. Prog Polym Sci 1999, 24, 185.
7. Vöit, B. J Polym Sci Part A: Polym Chem 2000, 38, 2505.
8. Kou, H. G.; Shi, W. F. Acta Polym Sin 2000, 5, 554.
9. Dzunuzovic, E.; Tasic, S.; Bozic, B.; Babic, D.; Dunjic, B. Prog Org Coat 2005, 52, 136.
10. Kim, Y. H.; Webster, O. W. Polym Prepr 1988, 29, 310.
11. Kim, Y. H.; Webster, O. W. J Am Chem Soc 1990, 112, 4592.
12. Wang, S. J.; Fan, X. D.; Si, Q. F.; Kong, J.; Liu, Y. Y.; Qiao, W. Q.; Zhang, G. B. J Appl Polym Sci 2006, 102, 5818.
13. Yan, D.; Gao, C. Macromolecules 2000, 33, 7693.
14. Jikei, M.; Kakimoto, M. A. Prog Polym Sci 2001, 26, 1233.
15. Wideman, T.; Fazen, P. J.; Su, K.; Remsen, E. E.; Zank, G.; Sneddon, L. G. Appl Organometal Chem 1998, 12, 681.
16. Bill, J.; Aldinger, F. Adv Mater 1995, 7, 775.
17. Lang, H.; Lühmann, B. Adv Mater 2001, 13, 1523.
18. Kroke, E.; Li, Y. L.; Konetschny, C.; Lecomte, E.; Fasel, C.; Riedel, R. Mater Sci Eng R 2000, 26, 97.
19. Cranat, P.; Pudas, M.; Hormi, O.; Hagberg, J.; Leppavuori, S. Carbohydr Polym 2004, 57, 225.
20. Wei, H.; Lu, Y.; Shi, W.; Yuan, H.; Chen, Y. J Appl Polym Sci 2001, 80, 51.
21. Kong, J.; Fan, X. D.; Zhang, G. B.; Xie, X.; Si, Q. F.; Wang, S. J. Polymer 2006, 47, 1519.
22. Karstedt, B. D. U.S. Pat. 3,775,452, (1973).
23. User Handbook of Photo Calorimeter Accessory; Waters-TA: USA, 2003, p 21.
24. Miravet, J. F.; Fréchet, J. M. J. Macromolecules 1998, 31, 3461.
25. Si, Q. F.; Wang, X.; Fan, X. D.; Wang, S. J. J Polym Sci Part A: Polym Chem 2005, 43, 1883.
26. Drohmann, C.; Möller, M.; Gorbatsevich, O. B.; Muzafarov, A. M. J Polym Sci Part A: Polym Chem 2000, 38, 741.
27. Buschbeck, R.; Lang, H. Inorg Chem Commun 2004, 7, 1213.
28. Wang, S. J.; Fan, X. D.; Liu, X.; Kong, J.; Liu, Y. Y.; Wang, X. Polym Intern 2007, 56, 764.
29. Yoon, K.; Son, D. Y. Macromolecules 1999, 32, 5210.
30. Wang, S. J.; Fan, X. D.; Kong, J.; Liu, Y. Y.; Zhang, G. B. Acta Polym Sin 2006, 8, 1024.
31. Hook, R. J. J Non-Cryst Solids 1996, 195, 1.
32. Hölter, D.; Burgath, A.; Frey, H. Acta Polym 1997, 48, 30.
33. Grcev, S.; Schoenmakers, P.; Ledema, P. Polymer 2004, 45, 39.
34. Tarazona, M. P.; Saiz, E. J Biochem Biophys Methods 2003, 56, 95.
35. Kong, J.; Fan, X. D.; Si, Q. F.; Zhang, G. B.; Wang, S. J.; Wang, X. J Polym Sci Part A: Polym Chem 2006, 44, 3930.
36. Yu, Y.; DesLauriers, P. J.; Rohlfing, D. C. Polymer 2005, 46, 5165.
37. Jaumann, M.; Rebrov, E. A.; Kazakova, V. V.; Muzafarov, A. M.; Goedel, W. A.; Möller, M. Macromol Chem Phys 2003, 204, 1014.
38. Simon, P. F. W.; Müller, A. H. E.; Pakula, T. Macromolecules 2001, 34, 1677.
39. Vöit, B. J Polym Sci Part A: Polym Chem 2005, 43, 2679.
40. Boey, F. Y. C.; Qiang, W. Polymer 2000, 41, 2081.
41. Cho, J. D.; Hong, J. W. Eur Polym J 2005, 41, 367.
42. Iojoiu, C.; Abadie, M. J. M.; Harabagiu, V.; Pinteala, M.; Simionescu, B. C. Eur Polym J 2000, 36, 2115.
43. Ruiz, C. S. B.; Machado, L. D. B.; Volponi, J. E.; Pino, E. S. Nucl Instr Meth Phys Res B 2003, 208, 309.
44. Lecamp, L.; Youssef, B.; Bunel, C. Polymer 1997, 38, 6089.
45. Maffezzoli, A.; Terzi, R. Thermochim Acta 1998, 321, 111.
46. Jiang, X.; Xu, H.; Yin, J. Polymer 2004, 45, 133.
47. Atai, M.; Watts, D. C. Dent Mater 2006, 22, 785.
48. Kamal, M. R.; Sourour, S. Polym Eng Sci 1973, 13, 59.
49. Kamal, M. R. Polym Eng Sci 1974, 14, 231.